

Numerical Stimulation of Welded Joints of Aa 5059 and Aa7079 During Friction Stir Welding Process

¹Mohankumar. K, ²Pugazhenth. R

¹Research Scholar, Department of Mechanical Engineering, VISTAS, Chennai, India

²Professor, Department of Mechanical Engineering, VISTAS, Chennai, India

mohan9841718420@gmail.com, pugal4@gmail.com

ARTICLE INFO

Received: 27 Jan 2025

Revised: 28 March 2025

Accepted: 12 Apr 2025

ABSTRACT

Introduction: In this present studies 6mm, thick AA 5059 and AA 7079 plates are friction stir welded at different tool rotational speeds of 500, 750 and 1000 rpm, with a circular, taper cylinder and threaded taper cylinder tools.

Objective: The ANSYS model analysis is done in FSW process and the various temperature distributions during different travel time values are evaluated and find the optimal configuration is identified by the numerical simulation.

Methods: The identified condition is applied to the friction stir welding process and experiments are carried out with the transverse speed of 40 mm/min of the tool.

Results: Vickers hardness test, microstructure analysis is performed on the welded material. Scanning Electron Microscopy (SEM) and Microhardness is done to identify the metallography studies.

Discussion: The findings from these investigations are presented and discussed.

Keywords: FSW, AA 5059, AA 7079, Numerical simulation, ANSYS, SEM

INTRODUCTION

The finite element analysis is a numerical technique used to solve complex engineering problems by dividing them into smaller, simpler parts or elements. ANSYS is a popular commercial software suite that provides a comprehensive range of tools for FEA and computational fluid dynamics (CFD) simulations [1-3]. The software is widely used in the aerospace, automotive, and manufacturing industries to design, simulate, and analyze various structures and systems [4]. In ANSYS, FEA is performed by dividing the structure or system into finite elements, each of which has a finite size and shape. The properties of each element, such as its material properties, geometry, and boundary conditions, are defined by the user [5]. The software then uses these properties to solve a system of equations that describes the behavior of the structure or system under various loads and conditions.

The ANSYS software suite includes several modules, each of which is designed to simulate different types of structures and systems. For example, the ANSYS Mechanical module is used for structural analysis, while the ANSYS Fluent module is used for fluid dynamics simulations. Other modules, such as ANSYS Electronics and ANSYS Multiphysics, are designed for simulating electromagnetic and multiphysics problems, respectively [6-9]. In addition to FEA, ANSYS also includes several tools for pre-and post-processing of simulation data. These tools enable users to define the geometry of the structure, create and mesh the finite elements, define boundary conditions, and analyze the simulation results [10-12]. The software also includes visualization tools to help users interpret and communicate the simulation results.

NUMERICAL SIMULATION OF FSW IN ANSYS

Numerical simulations of the FSW process can provide valuable insights into the material flow, temperature distribution, and other key factors that affect the quality of the weld [13]. The numerical simulation of the FSW process is typically performed using finite element analysis (FEA) software, such as ANSYS. The simulation is divided into two phases: pre-processing and analysis. In the pre-processing phase, the geometry of the FSW joint is modeled

and meshed into finite elements [14]. The material properties, boundary conditions, and welding parameters such as tool rotation speed and traverse speed are defined.

In the analysis phase, the FEA software solves a system of equations that describe the material flow, temperature distribution, and other parameters during the FSW process [15]. The simulation results provide information about the heat-affected zone, plastic deformation, and residual stresses in the weld. Several factors can affect the accuracy of FSW numerical simulations. These include the choice of material model, the mesh size, and the numerical methods used to solve the equations. Therefore, it is important to carefully select the appropriate models and parameters to ensure accurate results [16]. The numerical simulation of the FSW process can provide valuable insights into the material flow, temperature distribution, and other factors that affect the quality of the weld. FEA software, such as ANSYS, can be used to perform the simulations, but careful consideration should be given to the choice of material models and numerical parameters to ensure accurate results [17].

MATERIALS AND METHODS

AA 5059 is an Al-Mg alloy and primarily alloyed with magnesium. It is not strengthened by heat treatment, instead becoming stronger due to strain hardening, or cold mechanical working of the material [18]. The heat treatment doesn't strongly affect the strength, 5059 can be readily welded and retain most of its mechanical strength. Aluminium 7079 is an alloy that has a wide range of applications [19, 20]. From its corrosion resistance to its heat resistance and from its machining capabilities to its welding ability, aluminum 7079 is a versatile material used in many industries [21, 22].

Table 1 Conditions applied for the analysis in ANSYS

TOOL PROFILE	TOOL SPEED (rpm)
Circular	500
	750
	1000
Taper Cylinder	500
	750
	1000
Threaded Taper cylinder	500
	750
	1000

RESULT AND DISCUSSION

FSW analysis CASE 1: Tool Profile: Circular at Tool Speed 500 Rpm

Experimental work was carried out for the dissimilar Aluminium alloys AA 5059 and AA 7079 to perform the FSW techniques was designed with the aid of a solid modeling software CREOSOFTE, with a dimension of 100mm x 50mm x 5mm plates were designed. A non-consumable tool with various pin profiles of circular, taper cylindrical, threaded taper cylinders with a length of 4.75 mm was designed along with an outer shoulder diameter of 20 mm and inner shoulder diameter of 12 mm. With the help of ANSYS software analysis was carried out for dissimilar Aluminium alloys AA 5059 and AA 7079 welded plates with varying parameters of tool rotational speed of 500 rpm, with a tool pin profile of circular pin stress, strain, and deformation was analyzed by applying von-mises theory, analysis is carried out in each and every step and position of a tool plunging in the plates and travels along the plates in the traverse direction.

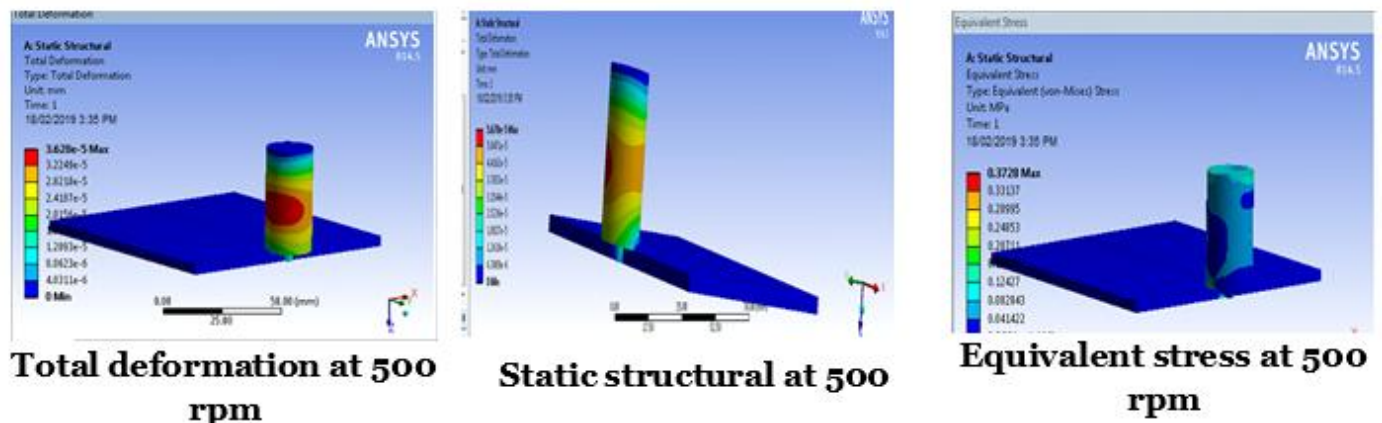


Fig. 1. FWS simulation analysis is carried for the of circular tool at 500 rpm

FSW analysis CASE 2: Tool Profile: Circular at Tool Speed 750 Rpm

The analysis carried out by ANSYS software analysis was carried out for dissimilar Aluminium alloys AA 5059 and AA 7079 welded plates with varying parameters of tool rotational speed of 750 rpm, with a tool pin profile of circular pin stress, strain, and deformation were analyzed by applying von-mises theory, analysis is carried out in every step and position of a tool plunging in the plates and travels along the plates in the traverse direction.

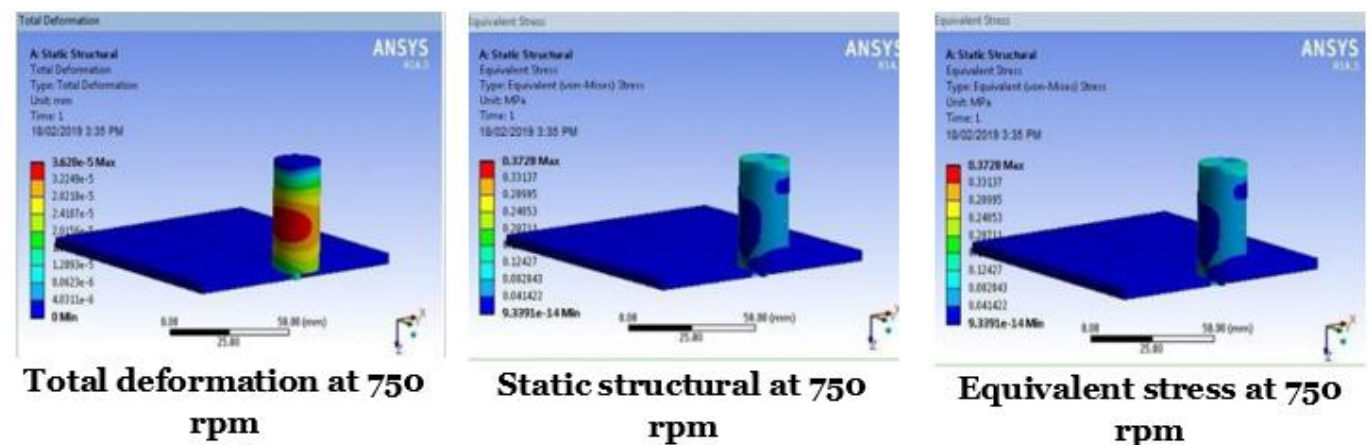


Fig. 2. FWS simulation analysis is carried for the of circular tool at 750 rpm

FSW Analysis CASE 3: Tool Profile: Circular at Tool Speed 1000 Rpm

Dissimilar Aluminium alloys AA 5059 and AA 7079 plates were joined with a tool rotational speed of 1000 rpm, with a tool pin profile of circular pin stress, strain, and deformation were analysis by applying von-mises theory, analysis are carried out in each and every step and position of a tool plunging in the plates and travels along the plates in traverse direction by using the ANSYS software.

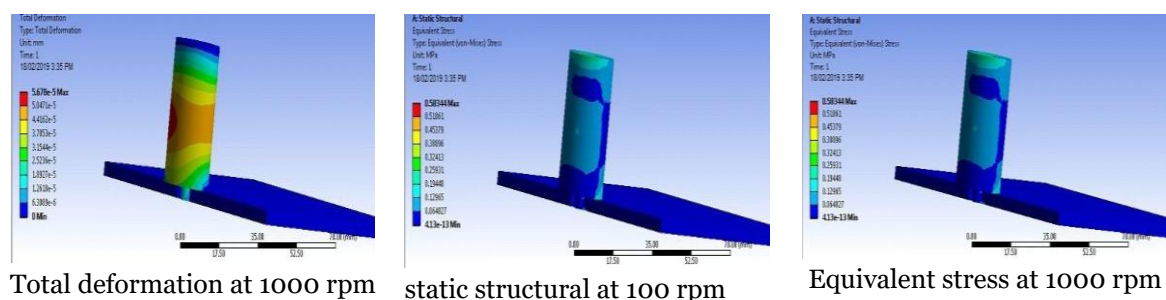


Fig. 3. FWS simulation analysis is carried for the of circular tool at 1000 rpm

FSW Analysis Case 4: Tool Profile: Taper Cylinder at Tool Speed 500 rpm

AA alloys AA 5059 and AA 7079 plates were joined with a tool rotational speed of 500 rpm, with a tool pin profile of Taper Cylinder pin stress, strain, and deformation were analyzed by applying von-mises theory, analysis is carried out in each and every step and position of a tool plunging in the plates and travels along the plates in traverse direction by using the ANSYS software.

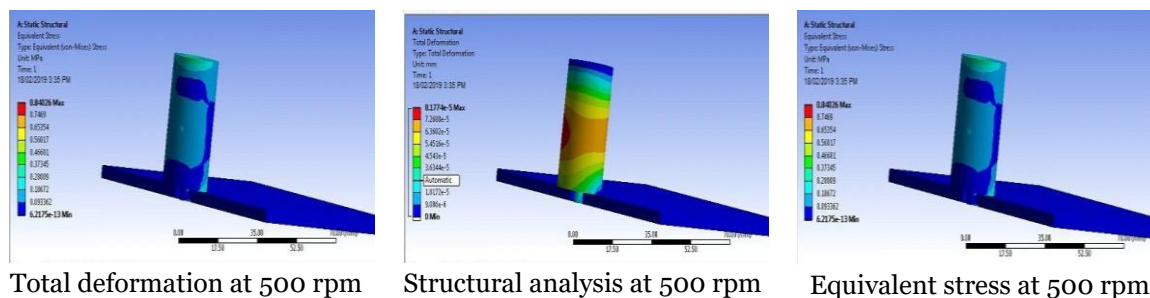


Fig. 4. FWS simulation analysis is carried for the of Taper Cylinder tool at 500 rpm

FSW Analysis Case 5: Tool Profile: Taper Cylinder at Tool Speed 750 rpm

Aluminium alloys AA 5059 and AA 7079 plates were joined with a tool rotational speed of 750 rpm, with a tool pin profile of Taper Cylinder pin stress, strain, and deformation were analyzed by applying von-mises theory, analysis is carried out in each and every step and position of a tool plunging in the plates and travels along the plates in traverse direction by using the ANSYS software.

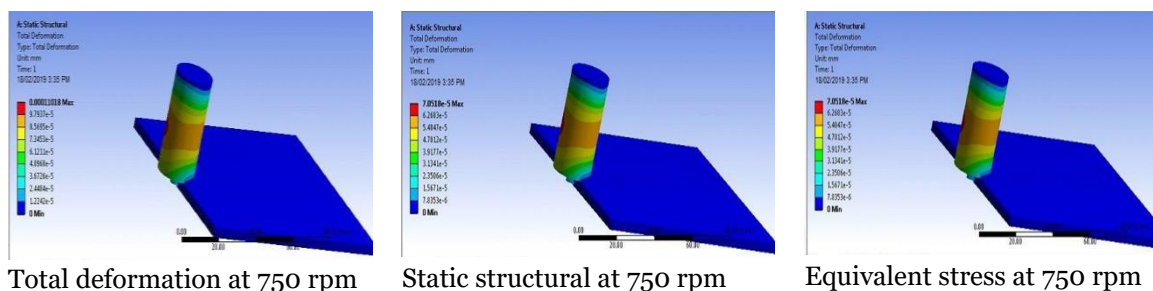


Fig. 5. FWS simulation analysis is carried for the of Taper Cylinder tool at 750 rpm

FSW Analysis Case 6: Tool Profile: Taper Cylinder at Tool Speed 1000 rpm

Aluminium alloys AA 5059 and AA 7079 plates were joined with a tool rotational speed of 1000 rpm, with a tool pin profile of Taper Cylinder pin stress, strain, and deformation were analyzed by applying von-mises theory, analysis is carried out in each and every step and position of a tool plunging in the plates and travels along the plates in traverse direction by using the ANSYS software.

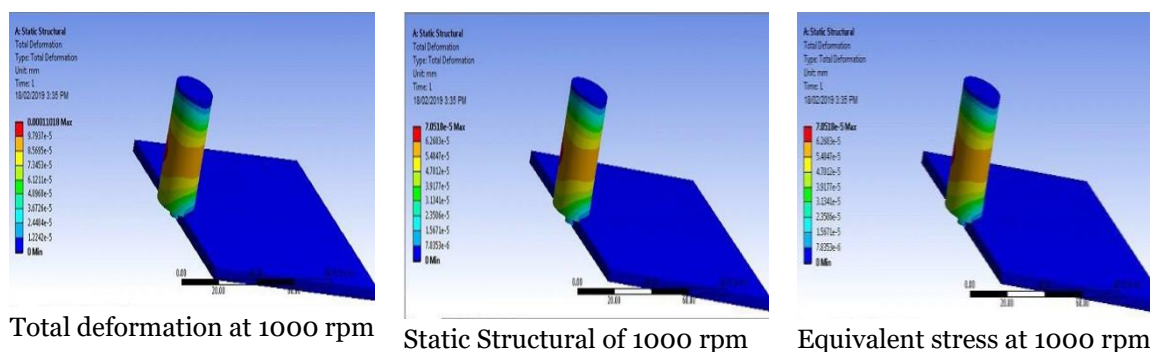
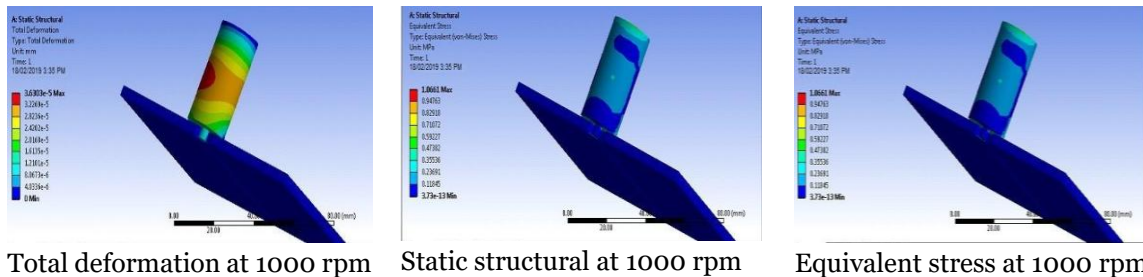


Fig. 6. FWS simulation analysis is carried for the of Taper Cylinder tool at 1000 rpm

FSW Analysis Case 7: Tool Profile: Threaded Taper Cylinder at Tool Speed 500 rpm

Aluminium alloys AA 5059 and AA 7079 plates were joined with a tool rotational speed of 500 rpm, with a tool pin profile of Threaded Taper Cylinder pin stress, strain, and deformation were analyzed by applying von-mises theory, analysis is carried out in every step and position of a tool plunging in the plates and travels along the plates in traverse direction by using the ANSYS software.



Total deformation at 1000 rpm

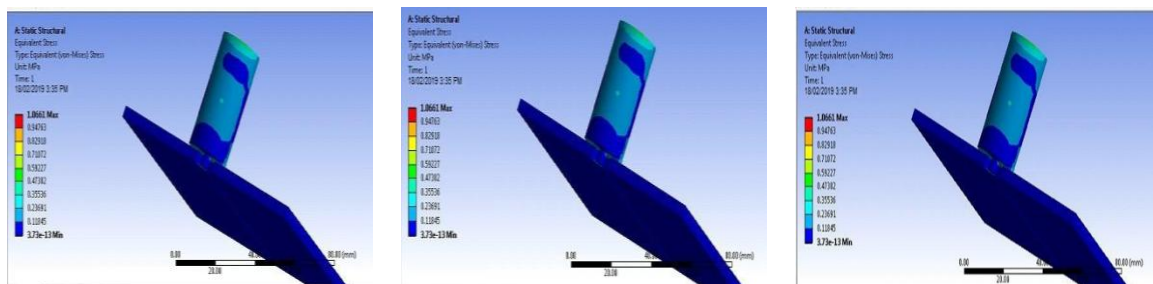
Static structural at 1000 rpm

Equivalent stress at 1000 rpm

Fig. 7. FWS simulation analysis for the of Threaded Taper Cylinder tool at 1000 rpm

FSW Analysis Case 8: Tool Profile: Threaded Taper Cylinder at Tool Speed 750 rpm

Aluminium alloys AA 5059 and AA 7079 plates were joined with a tool rotational speed of 750 rpm, with a tool pin profile of Threaded Taper Cylinder pin stress, strain, and deformation were analyzed by applying von-mises theory, analysis is carried out in every step and position of a tool plunging in the plates and travels along the plates in traverse direction by using the ANSYS software.



Total deformation at 750 rpm

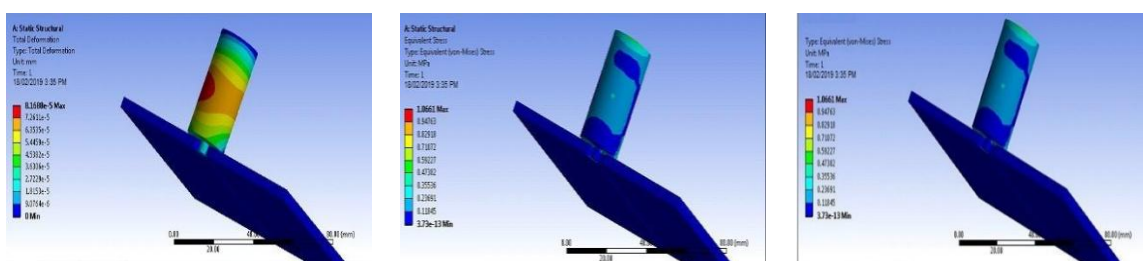
static structural at 750 rpm

Equivalent stress at 750 rpm

Fig. 8. FWS simulation analysis for the of Threaded Taper Cylinder tool at 750 rpm

FSW Analysis Case 9: Tool Profile: Threaded Taper Cylinder at Tool Speed 1000 rpm

Aluminium alloys AA 5059 and AA 7079 plates were joined with a tool rotational speed of 1000 rpm, with a tool pin profile of Threaded Taper Cylinder pin stress, strain, and deformation were analyzed by applying von-mises theory, analysis is carried out in every step and position of a tool plunging in the plates and travels along the plates in traverse direction by using the ANSYS software.



Static structural 1000 rpm

Equivalent stress at 1000 rpm

Total deformation at 1000 rpm

Fig. 9. FWS simulation analysis for the of Threaded Taper Cylinder tool at 1000 rpm

Table 2 Results in FSW of the MATERIAL- AA 5059 and AA 7079

TOOL PI PROFILE	TOOL SPEED (RPM)	DEFORMATION (mm)	STRESS (N/mm ²)	STRAIN
ROUND	500	3.26e-5	0.3728	5.381e-6
	750	5.678e-5	0.58344	8.421e-6
	1000	8.177e-5	0.84026	1.212e-5
Taper Cylinder	500	3.643e-5	0.38742	6.2753e-6
	750	5.528e-5	0.58792	9.523e-6
	1000	7.962e-5	0.84671	1.3715e-5
Threaded Taper cylinder	500	3.632e-5	0.41625	6.1856e-6
	750	5.675e-5	0.520036	9.464e-6
	1000	8.173e-5	0.93664	1.3919e-5

PROCESS PARAMTERS OF WELDED PARAMETERS

The Aluminium alloys of AA 5059 and AA 7079 and were joined by friction stir welding process for the above nine combination which is generated by Taguchi L9 orthogonal array. Table 3 shows the Process parameters, levels with responses of Ultimate Tensile strength, Yield Strength and % Elongation.

Table 3 Process parameters, levels with responses

E.No.	Rotational Speed (rpm)	Tool Traversing Speed (mm/sec)	Axial Force (kN)	Ultimate Tensile strength	Yield Strength	% Elongation
1	500	0.5	2	18	28	4.68
2	500	1	4	225	130	4.81
3	500	1.5	6	218	126	4.5
4	750	0.5	4	238	143	4.97
5	750	1	6	229	135	4.98
6	750	1.5	2	206	115	4.27
7	1000	0.5	6	231	136	4.73
8	1000	1	2	228	134	4.87
9	1000	1.5	4	221	134	4.69

ULTIMATE TENSILE FSW SPECIMENS

From the experimental results the highest Ultimate Tensile strength value of 238 N/m² is obtained by Rotational Speed 750 rpm, Tool Traversing Speed 0.5 mm/sec with Axial Force 4 kN and the highest yield strength of 143 also occurs on the same point of friction stir welding N m⁻². The lowest percentage of elongation occurs at Rotational Speed 750 rpm, Tool Traversing Speed 1.5 mm/sec with Axial Force 2 kN.

SEM IMAGES OF ULTIMATE TENSILE FSW SPECIMENS

The mechanical portions of the imperfection-free welds (created at 500–1000 rpm) to those of the two various parent essence. AA5059 and AA 7079 mixes of aluminium alloy. Figure 10 demonstrates that all disfigurement-free welds exhibit advanced tensile strength and extension values when compared to the other parent essence, the AA 7079 amalgamation, but lower strength and extension values when compared to the AA5059 amalgamation. They suggested that the primary cause of this ductile-brittle transition is a medium that strengthens grain boundaries. According to Figure 6, the welds created at 750 rpm primarily fractured in the AA5059 amalgamation to determine essence region, and the maturity of the tensile test samples has cracks in their lower hardness regions.

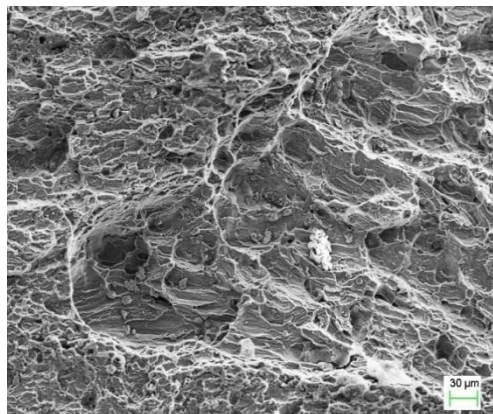


Fig. 10 SEM image of tensile fractured of FSW tool speed at 500 rpm

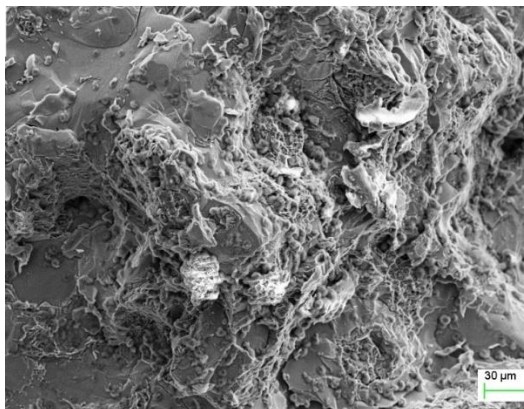


Fig. 11 SEM image of tensile fractured of FSW tool speed at 750 rpm

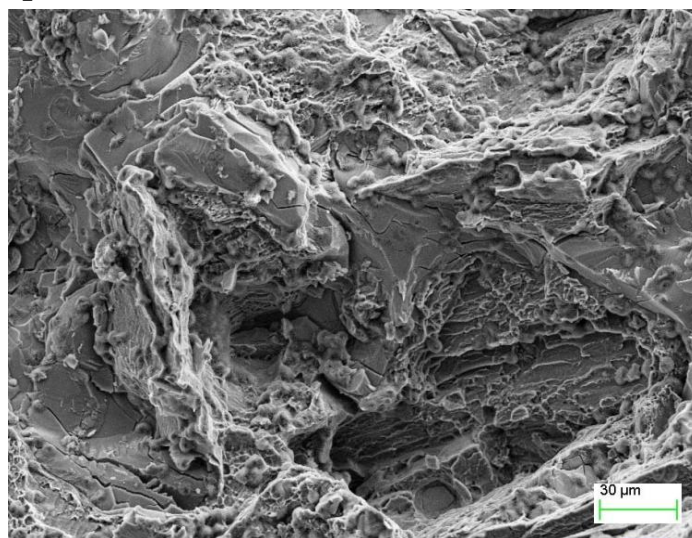


Fig. 12 SEM image of tensile fractured of FSW sample in tool speed at 1000 rpm

The fracture occurs inside the HAZ along the AA 7079 parent essence site as the fabrication is completed at 1000 rpm. Tensile fractured welds made at tool rotational speeds of 500, 750, and 1000 rpm are shown in figure 11. All of the tensile fracture shells can be seen in these photos to have checks and dents, proving that all of the welds failed in a ductile fashion. The fine dimples and regions with fractionalization-type fractures with properly positioned saw-toothed shells in the right places shown in the SEM images. Figure 12 shows the SEM image of tensile fractured of FSW sample in tool speed at 1000 rpm. Only after the metal has undergone homogenous material flow does this pattern of fracture appear. It is only possible to establish a uniform flow of metals during FSW of joints when the NZ

is totally defect-free. The tool's rotating speed was calibrated to affect modifications inside the loose joints' mechanical components.

CONCLUSION

In this research work a detailed FEA analysis were made for the configuration of AA 5059 and AA 7079 plates are friction stir welded in different tool rotational speeds of 500, 750 and 1000 rpm, with a circular, taper cylinder and threaded taper cylinder tools with the help of ANSYS. The plate thickness is taken as 6mm with transverse speed of 40 mm/min of the tool from the analysis optimal configuration is selected and experiments are carried out. Vickers hardness test, microstructure analysis is performed on the welded material. Scanning Electron Microscopy (SEM) and Microhardness is done to identify the metallography studies. The findings from these investigations are

- The numerical simulation analysis of ANSYS was conducted for three FSW tool pin profiles of circular, Taper cylinder, and Threaded Taper cylinders for three different tool speeds of 500 rpm, 750 rpm, and 1000 rpm.
- All the above three tool profiles and three speeds were taken into nine cases and they were analyzed. ANSYS analysis Threaded Taper cylinder performs better than the Taper cylinder and circular tool pin profiles for the Tool Speeds of 500 rpm and 750 rpm.
- The investigational study of the micro and SEM images revealed us that, the grains in the zone of stirring have been completely remodelled into homogenous, uniformly distributed, refined grains, which in turn contributed to the exceptional mechanical properties.

REFERENCE

- [1] Jeong, W., & Seong, J. (2014). Comparison of effects on technical variances of computational fluid dynamics (CFD) software based on finite element and finite volume methods. *International Journal of Mechanical Sciences*, 78, 19–26.
- [2] Zienkiewicz, O. C., Kelly, D. W., & Bettess, P. (1977). The coupling of the finite element method and boundary solution procedures. *International Journal for Numerical Methods in Engineering*, 11(2), 355–375.
- [3] Idelsohn, S. R., Onate, E., Calvo, N., & Del Pin, F. (2003). The meshless finite element method. *International Journal for Numerical Methods in Engineering*, 58(6), 893–912.
- [4] Kumar, S. D., Pugazhenth, R., Danial, S. A. A., & Swaminathan, G. (2021). Optimization of Dissimilar aluminum alloy by Friction stir welding Process Control variables with Multiple Objectives. *Journal of Physics: Conference Series*, 2040(1), 012042.
- [5] Grbović, A., & Mihajlović, D. (2017). Practical aspects of finite element method applications in dentistry. *Balkan Journal of Dental Medicine*, 21(2), 69–77.
- [6] Sabliov, C. M., Salvi, D. A., & Boldor, D. (2006). High frequency electromagnetism, heat transfer and fluid flow coupling in ANSYS multiphysics. *Journal of Microwave Power and Electromagnetic Energy*, 41(4), 5–17.
- [7] Variavel, M., Pugazhenth, R., & Jayakumar, V. (2018). Experimentation and simulation process of friction stir welding for lightweight similar and dissimilar materials. *MATEC Web of Conferences*, 172, 02012.
- [8] Bocchi, S., Cabrini, M., D'Urso, G., Giardini, C., Lorenzi, S., & Pastore, T. (2018). The influence of process parameters on mechanical properties and corrosion behavior of friction stir welded aluminum joints. *Journal of Manufacturing Processes*, 35, 1–15.
- [9] Chen, Y., Li, M., Yang, X., & Wei, K. (2020). Durability and mechanical behavior of CFRP/Al structural joints in accelerated cyclic corrosion environments. *International Journal of Adhesion and Adhesives*, 102, 102695.
- [10] Mohankumar, K., Pugazhenth, R., Khan, N. H., Srinivas, G. V. S., Parthiban, A., Karthick, M., ... & Majumder, H. (2024). Experimental investigation of the friction stir welding process of AA5059 and AA7079 and prediction using fuzzy approach. *Proceedings of the Institution of Mechanical Engineers, Part C: Journal of Mechanical Engineering Science*. <https://doi.org/10.1177/09544062241302529>
- [11] Vairavel, M., Pugazhenth, R., Kavitha, S., & Ganesan, K. (2020). Review of hybrid tool testing and measurement for friction stir welding. *European Journal of Molecular & Clinical Medicine*, 7(9), 2020.
- [12] Kangazian, J., & Shamanian, M. (2019). Micro-texture and corrosion behavior of dissimilar joints of UNS S32750 stainless steel/UNS N08825 Ni-based superalloy. *Materials Characterization*, 155, 109802.

- [13] Kumar, S. D., & Pugazhenth, R. (2023). Achievement of optimum characteristics of friction stir welded joints with varied process parameters. *International Journal of Vehicle Structures & Systems*, 15(5), 618–622.
- [14] Meyghani, B., Awang, M. B., Emamian, S. S., Mohd Nor, M. K. B., & Pedapati, S. R. (2017). A comparison of different finite element methods in the thermal analysis of friction stir welding (FSW). *Metals*, 7(10), 450.
- [15] Mironov, S. Y. (2023). Temperature distribution within the friction stir welding tool. *Physical Mesomechanics*, 26(1), 33–38.
- [16] Prabhakar, D. A. P., Korgal, A., Shettigar, A. K., Herbert, M. A., Chandrashekhara, M. P. G., Pimenov, D. Y., & Giasin, K. (2023). A review of optimization and measurement techniques of the friction stir welding (FSW) process. *Journal of Manufacturing and Materials Processing*, 7(5), 181.
- [17] Snihirova, D., Höche, D., Lamaka, S., Mir, Z., Hack, T., & Zheludkevich, M. L. (2019). Galvanic corrosion of Ti6Al4V-AA2024 joints in aircraft environment: Modelling and experimental validation. *Corrosion Science*, 157, 70–78.
- [18] Vijayan, D., & Abhishek, P. (2018). Multi Objective Process Parameters Optimization of Friction Stir Welding using NSGA-II. *IOP Conference Series: Materials Science and Engineering*, 390, 012012.
- [19] Tamjidy, M., Baharudin, B. T. H., Paslar, S., Matori, K. A., Sulaiman, S., & Fadaeifard, F. (2017). Multi-objective optimization of friction stir welding process parameters of AA6061-T6 and AA7075-T6 using a biogeography based optimization algorithm. *Materials*, 10(5), 533.
- [20] Vairavel, M., & Pugazhenth, R. (2021). Implementation of Computational Fluid Dynamics on Dissimilar Alloys for Friction Stir Welding Process. *Design Engineering*, 6578–6588.
- [21] Vijayan, D., & Seshagiri Rao, V. (2017). Optimization of friction stir welding process parameters using RSM based Grey-Fuzzy approach. *Saudi Journal of Engineering and Technology*, 2(1), 2–25.
- [22] Rahman, M. A., Kumar, S. D., & Pugazhenth, R. (2024). Design Optimization and Experimental Investigation on Friction Stir Welded Aluminium Alloys and its Mechanical Characteristics. *International Journal of Vehicle Structures & Systems*, 16(6).